Available online at www.sciencedirect.com

SciVerse ScienceDirect

Ceramics International 38 (2012) 5347–5354

CERAMICS INTERNATIONAL

www.elsevier.com/locate/ceramint

Improvement of barium titanate properties induced by attrition milling

M.M. Vijatović Petrović [a,*], J.D. Bobić [a], A.M. Radojković [a], J. Banys [b], B.D. Stojanović [a]

[a] *Institute for Multidisciplinary Research, Belgrade University, Kneza Viseslava 1, Serbia*
[b] *Faculty of Physics, Vilnius University, Sauletekio al. 9, Vilnius, Lithuania*

Received 28 February 2012; received in revised form 15 March 2012; accepted 15 March 2012
Available online 24 March 2012

Abstract

Barium titanate powder was prepared by soft chemical process from polymeric precursors (modified Pechini process). The synthesized barium titanate (BT) powder was nanosized and the factor of agglomeration (F_{agg}) pointed the existence of agglomerates. In order to de-agglomerate nanopowder and to enhance BT properties the attrition milling was performed. The milled powder (BTA) possessed smaller particles and the size and number of agglomerates was significantly reduced. To investigate the effect of milling on improvement of ceramics electrical properties, both BT and BTA powders were uniaxially pressed and sintered at 1300 °C for 8 h in air. The temperature dependence of relative permittivity showed three structural phase transitions for ferroelectric barium titanate ceramics. The dielectric constant at Curie temperature was ~6700 for BTA which is much higher than 1340, obtained for non-treated BT. The dielectric losses were below 0.04 in both BT ceramics. At higher temperatures the analysis of impedance measurements showed the presence of both grain interior and grain boundary effects. Much higher grain and grain boundary resistivities were obtained for the BTA ceramics.

Keywords: A. Powders: chemical preparation; B. Microstructure-final; B. Grain boundaries; C. Electrical properties

1. Introduction

Barium titanate is a ferroelectric material with a perovskite structure which has been of practical importance for over 60 years due to its specific electrical properties. Its great significance is based on possibility of wide application as ceramic capacitors, PTCR thermistors, piezoelectric sensors, optoelectronic devices, transducers, actuators, etc. [1,2]. Properties of ceramics are very sensitive to their microstructure, therefore the control of microstructure development is very important. In order to obtain ceramic materials with desired properties each step in the materials processing has to be monitored [3,4]. The most common factors that can influence the final properties of material are the agglomeration of powders influenced by a powder synthesis method, as well as the grain size and defects dependent on the processing method (type, temperature and time of sintering), additives, etc. [5,6].

During the years different types of synthesis methods were developed for barium titanate preparation. The advantage of chemical methods is the quasi-atomic dispersion of constituent components in a liquid precursor, which facilitates synthesis of crystallized powder with submicron particles and high purity [7]. The main problem that appears in chemically prepared powders is high agglomeration caused by very small primary particles that tend to join together. The agglomeration can have a high impact on the microstructure by forming non-uniform and coarse grained ceramics usually with exaggerated grains. This kind of microstructure can negatively affect the barium titanate electrical properties [2,4,8–11]. A possible way to reduce the number and dimensions of agglomerates is grinding of barium titanate powder in a specifically designed attrition mill.

Wet processing and dry grinding machines are available for obtaining the finest particles in the micron or even nanometer range with minimal contamination. For wet grinding in water, alcohol or organic solvents, agitator bead mills constructed of polyurethane, rubber or various ceramic materials are available, depending on the application [12].

Even though barium titanate based materials are widely investigated, there is still high interest for their research. Once the final properties of pure BT are tailored through obtaining pure and fine particle powders that produce uniform microstructure,

* Corresponding author. Tel.: +381 11 2085039; fax: +381 11 2085062.
E-mail address: miravijat@yahoo.com (M.M. Vijatović Petrović).

0272-8842/$36.00
doi:10.1016/j.ceramint.2012.03.041

doping of this material will be much easier allowing much wider application of BT. While many previous investigations showed how BT nanopowders can be obtained by different synthesis methods only a few are taking into account their high agglomeration that negatively affect materials properties.

The aim of this study is to show that properties of pure BT can be improved by attrition milling treatment for short period of time without evident contamination. The barium titanate nanopowder prepared by a chemical route was treated in the attrition mill with zirconia beads. The investigation of non-milled and milled powders and ceramics were carried out in order to see how the de-agglomeration of powder influenced the powder characteristics, development of ceramics microstructure and electrical properties.

2. Experimental work

The polymeric precursor method was used to obtain pure barium titanate powder. Barium and titanium citrate solutions were prepared using barium acetate and titanium-isopropoxide as a source of metal ions, Ba^{2+} and Ti^{4+}. The ratio between metal ion, citric acid and ethylene glycol was 1:4:16 in both solutions. The obtained citrates were mixed and heated at 140 °C for ~5 h, when the mixture changed into a brown glassy resin. The organic resin was decomposed during thermal treatments at 250 °C for 1 h and 300 °C for 4 h. It was noticed that the resin was transformed into a black solid mass (polymeric precursor) which was pulverized using an agate mortar and pestle. Further thermal treatment of precursor material was performed in the temperature range 350–800 °C/4 h and after that the nanopowder of barium titanate was formed (BT) [13,14].

Since the nanopowders obtained by chemical methods are usually highly agglomerated; such a powder was treated in attrition mill (PE075 Netzsch, Germany) with zirconia media for 1 h in 2% polyacrylic acid. The milled barium titanate powder (BTA) was dried at 150 °C and used for further investigation. In order to see the influence of attrition milling on barium titanate microstructure and electrical properties a complete analysis of the BT and BTA powders and ceramics was carried out.

The particle size distributions (PSDs) were measured using laser diffraction (Malvern Mastersizer S) and the specific surface areas (SSA) were obtained by nitrogen adsorption (Gemini 2375, Micromeritics). The average particle diameters (D_{BET}) were calculated from the SSA ($6/(\rho_{theoretical} \times SSA)$) and the factor of agglomeration was calculated by dividing D_{V50} and D_{BET}. The densities of barium titanate powders were measured using a He Pycnometer (Micromeritics AccuPyc 1330). The morphology of nanopowders was investigated by X-ray diffraction analysis (Cu Kα1, λ = 1.54059 Å, Model Phillips PW1710 diffractometer) and scanning electron microscopy (JEOL JSM-6610LV).

The nanopowders of BT and BTA were uniaxially pressed at 196 MPa into discs of 10 mm in diameter. The pallets were sintered at 1300 °C for 8 h in air with a heating rate of 10 °C/min in a tube furnace. The density of barium titanate ceramics was calculated geometrically. The phase purity and crystal structure was determined by XRD analysis using above mentioned diffractometer and SEM Tescan VEGA TS 5130MM was used for analysis of ceramic samples.

The measurements of dielectric properties were carried out using an LCR meter (model 4284 A, Hewllet-Packard) in the temperature range −175 to 175 °C and frequency range from 50 kHz to 1 MHz. Prior to the measurements the samples were prepared by applying Ag electrodes on the polished surfaces of the sintered ceramic discs. Since the values for real (ε') and imaginary (ε'') part of permittivity were determined experimentally, the dielectric loss tangent of barium titanate ceramics was calculated according to equation $\tan\delta = \varepsilon''/\varepsilon'$.

The impedance measurements were also carried out in the temperature range 250–500 °C with the step of 50 °C and in the frequency range 42 Hz to 1 MHz using HIOKI 3532-50 LCR HiTester. To obtain continuous metallic contacts, Pt paste was deposed on the polished surfaces of the BT and BTA ceramics. All collected data were analyzed using the commercial software package Z-view.

3. Results and discussion

The XRD analysis of the BT powder prepared by the modified polymeric precursor method is presented in Fig. 1. The presence of cubic barium titanate phase was found according to standard JCPDS files No. 31-0174. An average crystallite size was around 20–23 nm (calculated using Scherer's equation).

The results of the BT and BTA powders characterization using different analysis methods are presented in Table 1. The particle size distribution measurements indicated a high agglomeration of the starting BT powder and it can be clearly noticed from the calculated agglomeration factor. After attrition treatment for 1 h, the de-agglomeration of powders was evident. D_{V50} decreased rapidly and the factor of agglomeration was lowered for almost 85%. The specific surface area of barium titanate powder increased with milling, therefore, the reduction of the average particle size, D_{BET}, was also noticed. The SEM micrographs showed in Fig. 2 present barium titanate powders before and after milling with rounded primary particles ~40–60 nm. It is evident that with attrition milling the number and dimensions of agglomerates were diminished. The density of the obtained powders was 5.72 ± 0.02 g/cm^3.

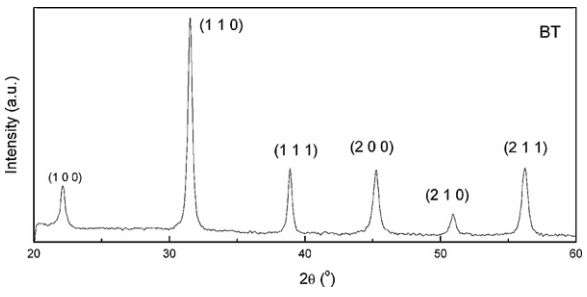

Fig. 1. X-ray diffractogram of pure barium titanate powder.

Table 1
Results obtained by characterization of BT and BTA powders.

Sample	D_{V10} (nm)	D_{V50} (nm)	D_{V90} (nm)	SSA (m^2/g)	D_{BET} (nm)	F_{agg} (nm)
BT	1920	6530	13,690	13.47	74	88
BTA	320	690	1510	19.91	50	14

The XRD data (Fig. 3) of the sintered samples indicate formation of barium titanate tetragonal crystal structure which is identified by appearance of its characteristic diffraction peaks (JCPDS files No. 05-0626). Since the milling was performed using zirconia beads it was assumed that the contamination of barium titanate is possible [15,16]. However, in the XRD data for the BTA ceramics only peaks that correspond to barium titanate tetragonal phase could be noticed. The calculated lattice parameters confirmed formation of the tetragonal structure in both samples. The ratio c/a for the starting BT material was 1.0053 but for the BTA ceramic was slightly lower than 1.0045, indicating the decrease of tetragonality with attrition treatment. These results are in agreement with data published for BT attrition milled powders obtained by the solid state reaction [15].

The microstructure of the ceramics showed formation of polygonal grains and microstructures with different grain size

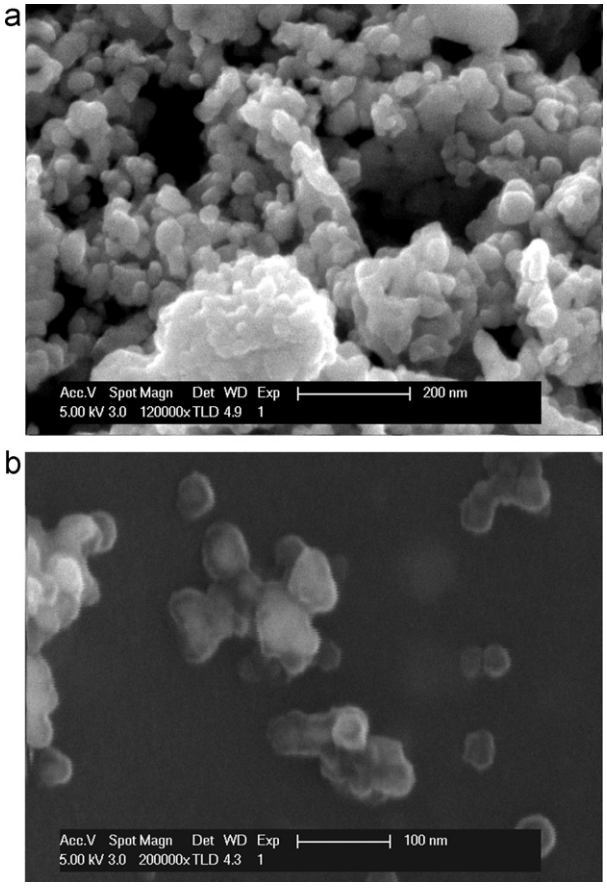

Fig. 2. SEM micrographs of BT and BT barium titanate powders (a) BT and (b) BTA.

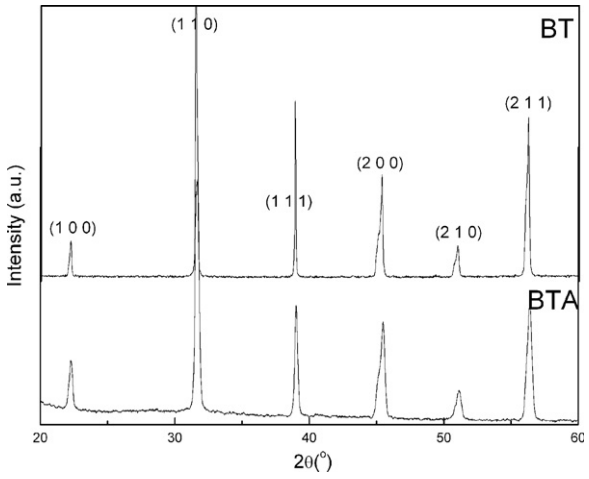

Fig. 3. X-ray diffractograms of BT and BTA samples sintered at 1300 °C/8 h.

distributions (Fig. 4). In the BT ceramics the grain size distribution was broader, from 2 to 5 μm but in the BTA ceramics the average grain size changes from 1.5 to 3 μm and the microstructure is more homogeneous than in the BT ceramics. These results are in agreement with the particle size distribution analysis of powders, where the coarser powders resulted in a larger-grained and coarse ceramic microstructure. The density of the BTA ceramics was ∼95% of theoretical value and it was higher than that obtained for the BT ceramics, ∼90%.

The dielectric properties of barium titanate ceramics are presented in Fig. 5. Dielectric anomalies that correspond to three structural transitions (cubic to tetragonal – T_{C-T}, tetragonal to orthorhombic – T_{T-O}, orthorhombic to rombohedral – T_{O-R}) could be detected in both ceramics on the curve typical for classical ferroelectric barium titanate material. Both exhibit sharp permittivity maximum at T_C but it is located at a slightly higher temperature for BTA around 123 °C compared to 120 °C found for BT. The dielectric permittivity value at Curie temperature increased from 1340 to 6700 after attrition milling (Table 2). Literature data [17–19] have shown that with a decrease in grain size the dielectric constant increases and that is in agreement with results obtained in our study. Furthermore, the possible factors that influence the ε' enhancement could be more homogeneous microstructure and higher density obtained for the BTA ceramics. On the other hand, the inclusion of Zr in BT lattice can affect the electrical properties of barium titanate [16,20]. It causes the broadening and flattering of ε'–T plots with appearance of diffuse phase transition at Curie temperature but in our study we obtained sharp T_C maximum for the BTA ceramics. Some authors had shown that Zr can influence the permittivity decrease and that is not the case for our ceramics. Thakur et al. noticed the contamination of barium titanate powders treated in attrition mill after 3 h of milling. They noticed in their ceramics all appearances previously mentioned [15].

The dielectric losses tangent as a function of temperature for both barium titanate ceramics is presented in Fig. 6. All three characteristic phase transitions could be noticed at the given

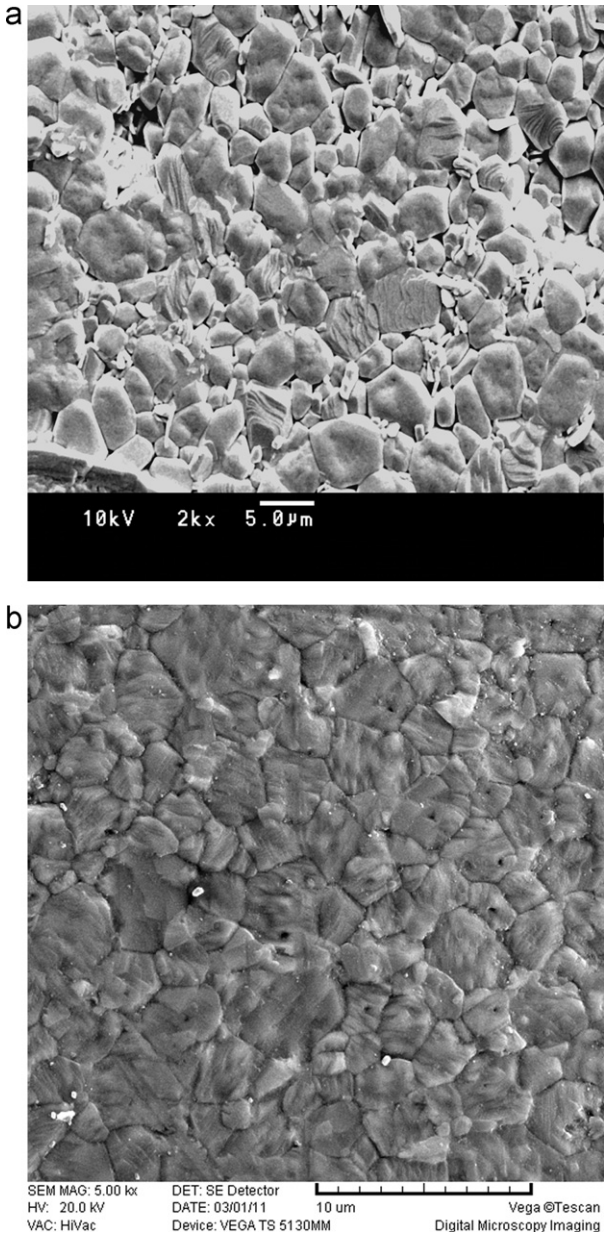

Fig. 4. Micrographs of barium titanate specimens sintered at 1300 °C for 8 h (a) BT and (b) BTA.

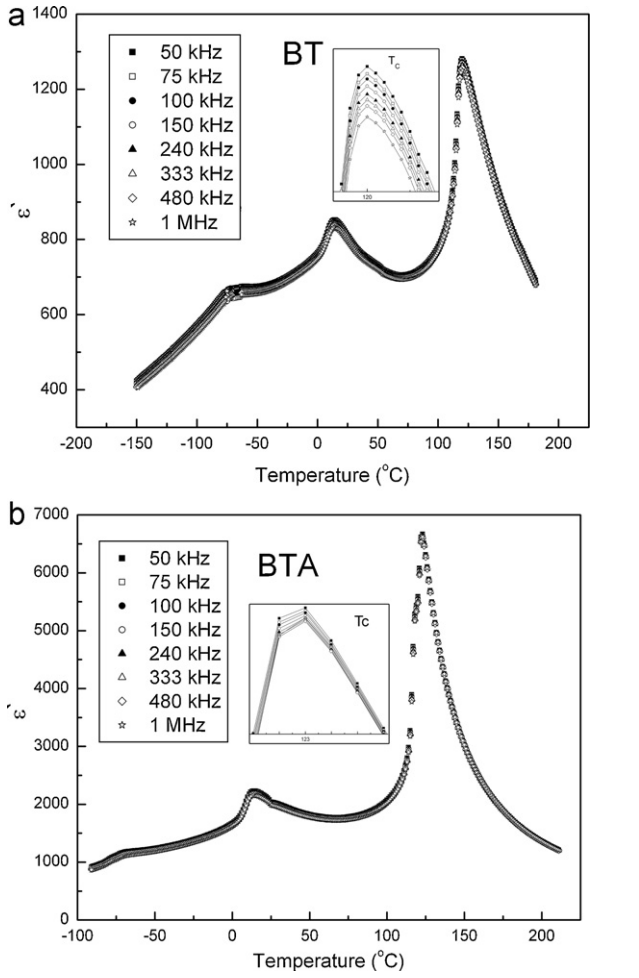

Fig. 5. Temperature dependence of dielectric constant in the frequency range from 50 kHz to 1 MHz for (a) BT and (b) BTA ceramics.

diagram. At higher temperatures the dielectric losses have shown the increase and frequency dispersion in paraelectric state that can be related to thermally activated Maxwell–Wagner relaxation [21,22]. Tan δ values were under 0.04 for both investigated ceramics in whole temperature range and below 0.02 at room temperature.

Table 2
Transition temperatures and dielectric constant values for all samples at 100 kHz.

Sample	T_{C-T} (°C)	T_{T-O} (°C)	T_{O-R} (°C)	ε' (T_{room})	ε' (T_C)	tan δ
BT	120	14	−74	872	1340	0.03
BTA	123	13	−73	2268	6700	0.02

Furthermore, the influence of frequency on the dielectric properties was investigated for both barium titanate ceramics in the frequency range from 20 to 10^6 Hz. The frequency dependence of the real and imaginary part of the permittivity in the temperature range 25–150 °C is shown in Fig. 7 and Fig. 8, respectively. The real part of permittivity of both ceramics showed the tendency of a slight decrease with frequency. In the case of BT ceramics, at lower temperatures the decrease in almost linear, but at higher temperatures there is a visible drop from 20 Hz up to 1 kHz. The BTA ceramics characterize a linear decrease of the dielectric permittivity in all frequency range for all investigated temperatures. The imaginary part of the permittivity showed frequency independence at lower temperatures, but at temperatures higher then 100 °C there is an increase in the lower frequency range for both ceramics. The insight into the relaxation of the real and imaginary dielectric permittivity have shown that there is non-Debye behavior due to the absence of typical broad Debye-like relaxation peak of $\varepsilon''(f)$ [22,23]. In general, the tendency of ε'' to increase with a frequency decrease indicates the onset of the Maxwell–Wagner effect [22,23]. Such a low frequency relaxation can have different origins and may be related to conductivity or to thermally activated space charge effects at

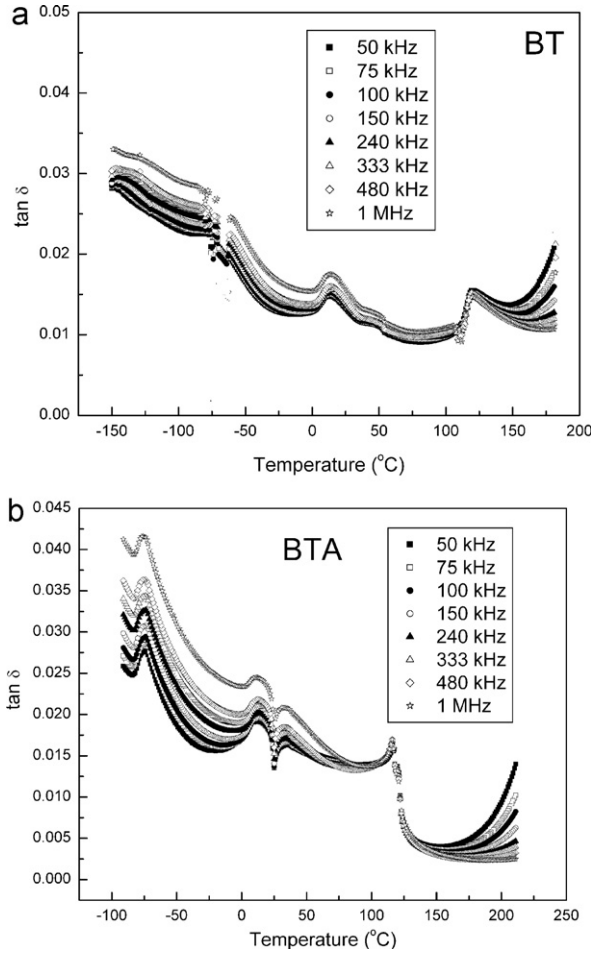

Fig. 6. Temperature dependence of dielectric losses in the frequency range from 50 kHz to 1 MHz for (a) BT and (b) BTA ceramics.

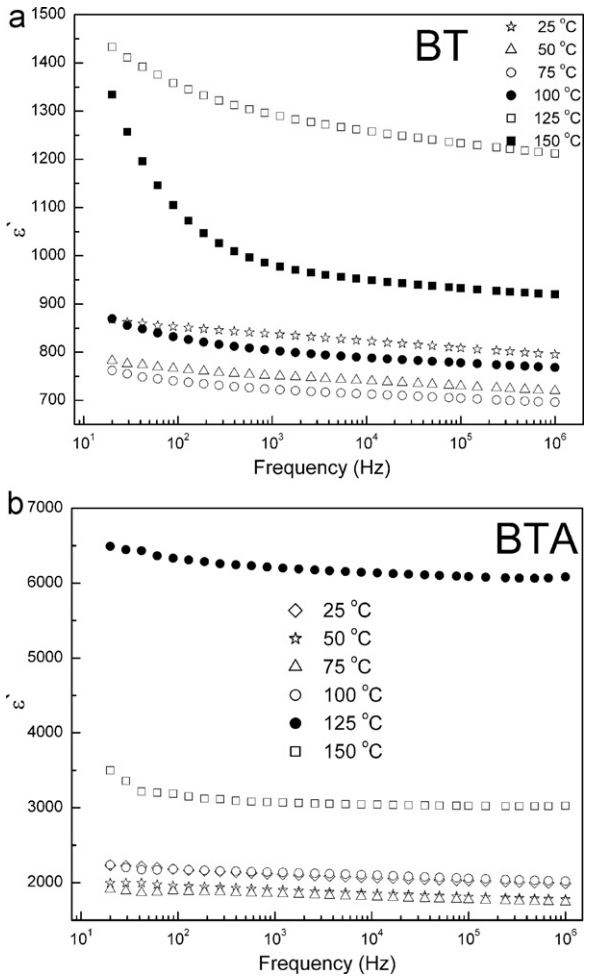

Fig. 7. (a) and (b) Frequency dependence of real part of permittivity barium titanate samples in the frequency range 20–10^6 Hz and temperature range 25–150 °C.

low frequencies (Maxwell–Wagner phenomena). It is assumed that this effect is closely connected with the presence of oxygen vacancies in the sintered ceramics or to small grain boundary electrical inhomogeneities [21,22].

The impedance spectroscopy (IS) was used to evaluate and separate the contributions of various components such as grain, grain boundary and electrode to the overall electrical properties of barium titanate ceramics. This analysis is a useful tool for the investigation of electrical homogeneity of the ceramics [24,25]. The results obtained from IS are presented in terms of impedance (Z) and modulus (M) formalisms. A major problem in the characterizing of pure barium titanate is that the resistivity is too high to be measured at the temperatures below 200 °C [24]. Therefore, the measurements in this study were carried out in the temperature range far above Curie temperature. The complex impedance plane plots of data collected in the temperature range 300–500 °C of the BT and BTA ceramics are presented in Fig. 9. Two well resolved semicircular arcs are observed in the plots recorded at 300 and 350 °C for the BT ceramics, and in the temperatures range 300–450 °C for the BTA samples. At higher temperatures there is depressed semicircle indicating possible overlapping of two semicircular arcs. It is suggested that the low frequency semicircle corresponds to the grain boundary contribution and the high frequency semicircular arc is attributed to the grain contribution. The absence of third semicircle suggests that the contribution of electrode-materials interface to impedance is negligible in the observed frequency range. Perhaps the measurements at much lower frequencies could enable the detection of this contribution. The equivalent circuit consisted of two parallel RC elements connected in series and Z-view fitting software was used to evaluate the values of R_g and R_{gb}. It is apparent from the extracted resistivity data (Table 3) that the attrition milling of powders causes the increase in grain and grain boundary resistivity of barium titanate ceramics. It is especially prominent in the temperature range from 300 to 400 °C. These results are in agreement with Thakur et al. study of barium titanate obtained by the solid state reaction which is also treated in attrition mill [15].

Arrhenius plots of the grain σ_g ($\sigma_g = 1/R_g$) and grain boundary σ_{gb} ($\sigma_{gb} = 1/R_{gb}$) conductivity for both ceramics are presented in Fig. 10. It can be noticed that they both obey the Arrhenius low expressed by the equation $\sigma = \sigma_o \exp(-E_a/k_BT)$ [26]. The activation energies for various conduction processes can be estimated from the slopes of the given diagrams. One can see that the E_a for both grain and grain boundary conductions of

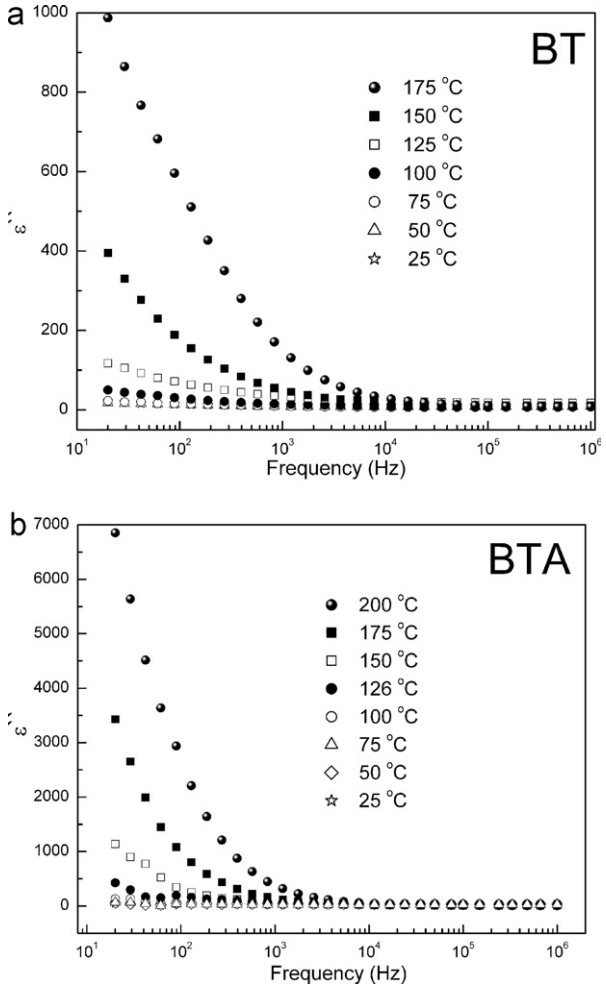

Fig. 8. (a) and (b) Frequency dependence of imaginary part of permittivity barium titanate samples in the frequency range 20–10^6 Hz and temperature range 25–150 °C.

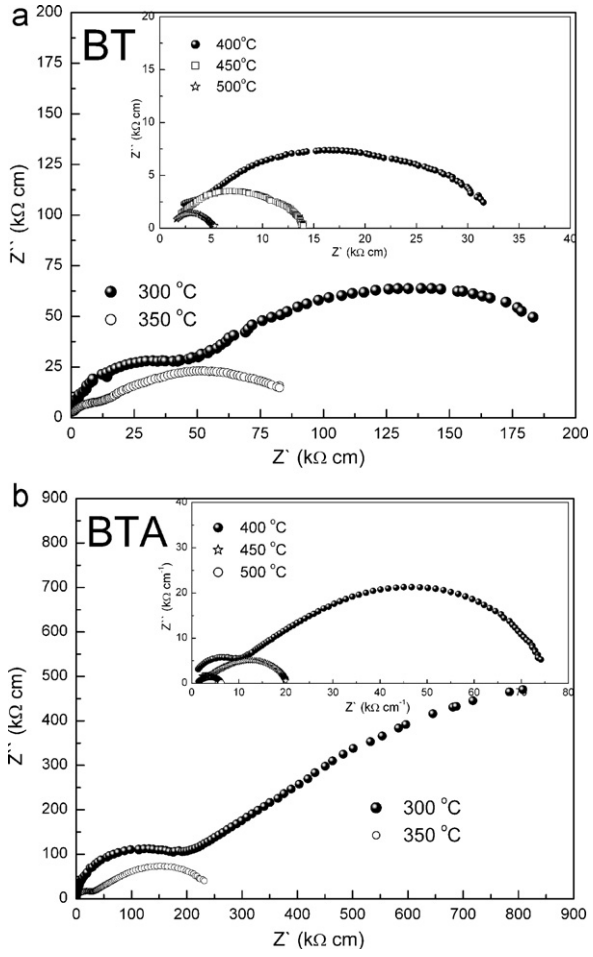

Fig. 9. The complex impedance plane plots in the temperature range 300–500 °C of (a) BT and (b) BTA ceramics.

the BTA ceramic were higher than that of the BT ceramic. The activation energy for the conduction process through the grain boundaries had higher values in both samples. Thus, it can be indicated that the dominant effect in total conduction of ceramics is the grain boundary effect. The band gap for intrinsic electronic conduction in pure barium titanate is ∼3.0 eV. However, when both activation energies (for grain and grain boundary conductions) are much smaller than a half of this value, σ_g and σ_{gb} are attributed to an extrinsic conduction mechanism [15,25,26]. In our investigation much lower values for the grain and grain boundary conductivities were obtained for both ceramics. The suggested extrinsic conduction mechanism could be caused by the presence of defects such as oxygen vacancies that are initially present in starting material. On the other hand, the decrease of σ_g and σ_{gb} with attrition milling could be related to possible ''filling'' of some oxygen vacancies influencing the lowering of carrier concentration in the ceramics or obtaining much thicker grain boundaries with high resistivity [15].

Table 3
Grain and grain boundary resistivities data obtained from impedance complex plane plots.

Sample	T (°C)	R_g (kΩ cm)	R_{gb} (kΩ cm)
BT	300	40.5	189
	350	8.31	92
	400	3.8	32
	450	2.1	11.6
	500	1.2	3.2
BTA	300	179	1270
	350	33.4	232
	400	12.2	67.1
	450	4.92	16.7
	500	1.41	3.64

In order to complement and verify the data obtained by fitting of impedance complex plane plots ($Z'' - Z'$) at different temperatures, the $Z'' - f$ and $M'' - f$ ($M'' = C_o\omega Z'$, where C_o is vacuum capacitance of the cell without sample, $\omega = 2\pi f$ is angular frequency, Z' real part of impedance) spectroscopic plots were used for the extraction of the grain and grain boundary resistivities and capacitances [27,28]. M'' spectra are dominated by the grain response, and M'' Debye-like peak can be used to calculate R_g (grain resistivity) and C_g (grain capacitance) using the following relationships, $C_g = \varepsilon_o/2M''_{max}$

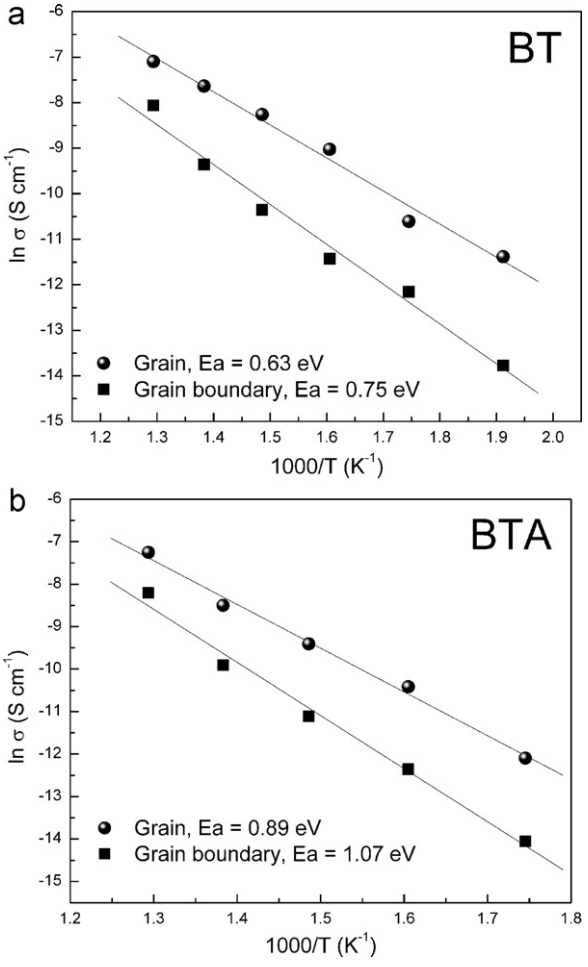

Fig. 10. Arrhenius plots of σ_g and σ_{gb} for (a) BT and (b) BTA ceramics.

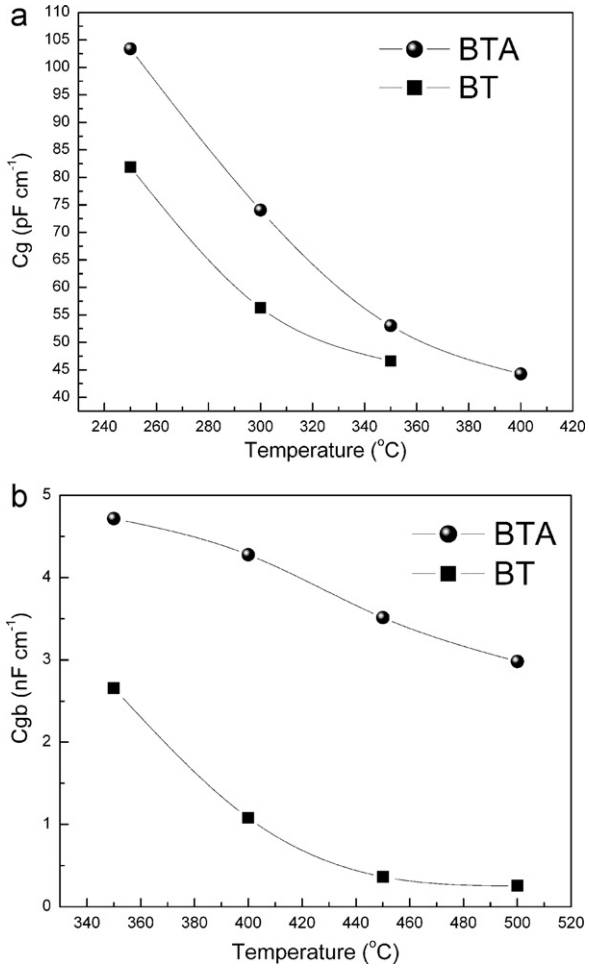

Fig. 11. Temperature dependence of C_g and C_{gb} for (a) BT and (b) BTA ceramics.

and $R_g = 1/2\pi f_{max} C_g$, where the f_{max} is the frequency at the top of M''_{max} Debye-like peak [26]. It was noticed that R_g increases significantly in the case of attrition milled powders.

On the other hand, Z'' spectra are dominated by the grain boundary response and Debye-like peak can be used to estimate R_{gb} (grain boundary resistivity) and C_{gb} (grain boundary capacitance) from the relationships, $R_{gb} = 2Z''_{max}$ and $C_{gb} = 1/2\pi f_{max} R_{gb}$, where the f_{max} is the frequency at the top of Z''_{max} Debye-like peak [26]. The main difference between the ceramics is that R_{gb} are much higher for the attrition treated ceramics indicating the formation of thick grain boundaries in a denser and more homogeneous sample which is evident also from the SEM micrographs [15].

The results for R_g and R_{gb} were used to evaluate the grain ($\sigma_g = 1/R_g$) and grain boundary ($\sigma_{gb} = 1/R_{gb}$) conductivities. It is important to point out that the activation energies determined in this way have shown similar values with those obtained from the complex impedance spectrum. From the values of the activation energies (for the BT, $E_{a(g)} = 0.59$ eV and $E_{a(g-b)} = 0.73$ eV and for the BTA, $E_{a(g)} = 0.88$ eV and $E_{a(g-b)} = 1.1$ eV) can be suggested again that the electrical responses could be attributed to the variation in oxygen vacancies content across the grain and grain boundary regions. It is known that oxygen vacancies in the perovskite ferroelectrics materials are considered as one of the mobile charge carriers and mostly in titanates, the ionization of oxygen vacancies creates conduction electrons [29]. Thus, the presented results suggest two parallel RC elements as a valid model for interpreting the IS spectra.

The temperature dependence of the grain and grain boundary capacitance for both BT and BTA ceramics are given in Fig. 11. The capacitances values showed descending dependence on the temperature in the BT and BTA ceramics as it is expected for ferroelectric materials above Curie temperature [30]. C_{gb} has higher value in comparison with C_g in both ceramics in whole temperature range, which is in accordance with the brick layer model for electroceramics that shows $C_{gb} \gg C_g$ [30]. On the other hand, the BTA ceramic has shown higher values of both types of capacitance compared to the BT ceramic indicating the formation of thicker grain boundaries that act as a barrier to the cross transport of the charge carriers.

This study has shown that the attrition milling for relatively short period of time (1 h) can influence barium titanate microstructure and therefore to improve the electrical properties without evident contamination.

4. Conclusion

The attrition milling of barium titanate powder for 1 h, which is relatively short period of time, has shown significant effect on barium titanate structure and its electrical properties. The de-agglomeration of starting powder and a certain lowering of the primary particle size (from 74 to 50 nm) and factor of agglomeration decreased from 88 for the BT to 14 for the BTA powder. Therefore, it was succeeded the formation of more homogeneous microstructure during the sintering. The dielectric permittivity of the BTA ceramics was much higher ∼6700 in comparison with 1340 obtained for the BT ceramics and it was frequently almost independent. The dielectric losses tangent was found to be lower than in the BT ceramics and below 0.02. The impedance spectroscopy analysis showed much higher grain and grain boundary resistivities, indicating also that $R_{gb} \gg R_g$. On the other hand, the obtained capacity appear to be higher in the attrition milled material showing $C_{gb} \gg C_g$ that is in agreement with brick layer model for the electroceramics with insulating grain boundaries. The equivalent circuit that consists of two parallel RC elements connected in series was found to be suitable for the investigated barium titanate ceramics. It was suggested that the presence of oxygen vacancies has the main influence on conduction processes in the grain and grain boundary regions.

The attrition milling of pure barium titanate is a very useful tool for obtaining pure and fine particles powders and ceramics with uniform microstructure and improved properties.

Acknowledgments

The authors gratefully acknowledge the Ministry of Education and Science of Republic of Serbia for the financial support of this work (projects III45021 and COST 539). Special thanks to Dr. Paul Bowen from EPFL, Lausanne, Switzerland for generous research support.

References

[1] F. Jona, G. Shirane, Ferroelectric Crystals, Dover Publications Inc., New York, 1993.
[2] A.J. Moulson, J.M. Herbert, Electroceramics, second ed., John Wiley & Sons Ltd., England, 2003.
[3] F.S. Shiau, T.T. Fang, T.H. Leu, Effects of milling and particle size distribution on the sintering behavior and the evolution of the microstructure in sintering powder compacts, Mater. Chem. Phys. 57 (1998) 33–40.
[4] S. Tusseau-Nenez, J.P. Ganne, M. Maglione, A. Morell, J.C. Niepce, M. Pate, BST ceramics: effect of attrition milling on dielectric properties, J. Eur. Ceram. Soc. 24 (2004) 3003–3011.
[5] S.M. Bobade, D.D. Gulwade, A.R. Kulkarni, P. Gopalan, Dielectric properties of A- and B-site doped $BaTiO_3$ (I): La- and Al-doped solid solution, J. Appl. Phys. 97 (2005) 074105.
[6] S. Tangjuanak, T. Tunkasiri, Characterization and properties of Sb-doped $BaTiO_3$ powders, Appl. Phys. Lett. 90 (2007) 072908.
[7] W.S. Cho, E. Hamada, Synthesis of ultrafine BaTiO3 particles from polymeric precursor: their structure and surface property, J. Alloys Compd. 266 (1998) 118–122.
[8] K. Niesz, T. Ould-Ely, H. Tsukamoto, D.E. Morse, Engineering grain size and electrical properties of donor-doped barium titanate ceramics, Ceram. Int. 37 (2011) 303–311.
[9] P. Balakrishna, B. Narasimha Murty, M. Anuradha, A new process based agglomeration parameter to characterize ceramic powders, J. Nucl. Mater. 384 (2009) 190–193.
[10] L. Dan, L. Zhongyang, Y. Chunjiang, C. Kefa, Study on agglomeration and densification behaviors of gadolinium-doped ceria ceramics, J. Rare Earth 25 (2007) 163–167.
[11] H.M. Lee, C.Y. Huang, C.J. Wang, Forming and sintering behaviors of commercial α-Al_2O_3 powders with different particle size distribution and agglomeration, J. Mater. Process. Technol. 209 (2) (2009) 714–722.
[12] http://www.netzsch-grinding.com/industries-applications/ceramics-glass/technical-ceramics.html, 2011.
[13] M.M. Vijatović, B.D. Stojanović, J.D. Bobić, T. Ramoška, P. Bowen, Properties of lanthanum doped $BaTiO_3$ produced from nanopowders, Ceram. Int. 36 (2010) 1817–1824.
[14] L. Ramajo, R. Parra, M. Reboredo, M. Zaghete, M. Castro, Heating rate and temperature effects on the $BaTiO_3$ formation by thermal decomposition of (Ba,Ti) organic precursors during the Pechini process, Mater. Chem. Phys. 107 (2008) 110–114.
[15] O.P. Thakur, A. Feteira, B. Kundys, D.C. Sinclair, Influence of attrition milling on the electrical properties of undoped-$BaTiO_3$, J. Eur. Ceram. Soc. 27 (2007) 2577–2589.
[16] P. Kumar, S. Singh, M. Spah, J.K. Juneja, C. Prakash, K.K. Raina, Synthesis and dielectric properties of substituted barium titanate ceramics, J. Alloys Compd. 489 (2010) 59–63.
[17] W. Luan, L. Gao, J. Guo, Size effect on dielectric properties of fine-grained $BaTiO_3$ ceramics, Ceram. Int. 25 (1999) 727–729.
[18] O.P. Thakur, C. Prakash, A.R. James, Enhanced dielectric properties in modified barium titanate ceramics through improved processing, J. Alloys Compd. 470 (2009) 548–551.
[19] L. Wu, M.C. Chure, K.K. Wu, W.C. Chang, M.J. Yang, W.K. Liu, M.J. Wu, Dielectric properties of barium titanate ceramics with different materials powder size, Ceram. Int. 35 (2009) 957–960.
[20] X.D. Betriu, J.E. Garcia, C. Ostos, A.U. Boya, D.A. Ochoa, L. Mestres, R. Perez, Phase transition characteristics and dielectric properties of rare-earth (La, Pr, Nd, Gd) doped $Ba(Zr_{0.09}Ti_{0.91})O_3$ ceramics, Mater. Chem. Phys. 125 (2011) 493–499.
[21] N. Horchidan, A. Ianculescu, L. Curecheriu, F. Tudorache, V. Musteata, S. Stoleriu, N. Dragan, D. Grisan, S. Tascu, L. Mitoseriu, Preparation and characterization of barium titanate stannate solid solutions, J. Alloys Compd. 509 (2011) 4731–4737.
[22] M.M. Vijatovic Petrovic, J.D. Bobic, T. Ramoska, J. Banys, B.D. Stojanovic, Antimony doping effect on barium titanate structure and electrical properties, Ceram. Int. 37 (2011) 2669–2677.
[23] D. O'Neill, R.M. Bowman, J.M. Gregg, Dielectric enhancement and Maxwell–Wagner effects in ferroelectric superlattice structure, Appl. Phys. Lett. 77 (2000) 1520–1522.
[24] A.R. West, D.C. Sinclair, N. Hirose, Characterization of electrical materials, especially ferroelectrics by impedance spectroscopy, J. Electroceram. 1 (1) (1997) 65–71.
[25] S. Devi, A.K. Jha, Phase transition and electrical characteristics of tungsten substituted barium titanate, Physica B 404 (2009) 4290–4294.
[26] F.D. Morrison, D.C. Sinclair, A.R. West, Characterization of lanthanum-doped barium titanate ceramics using impedance spectroscopy, J. Am. Ceram. Soc. 84 (3) (2001) 531–538.
[27] N. Hirose, A.R. West, Impedance spectroscopy of undoped $BaTiO_3$ ceramics, J. Am. Ceram. Soc. 79 (6) (1996) 1633–1641.
[28] A. Shukla, R.N.P. Choudhary, A.K. Thakur, D.K. Pradhan, Structural, microstructural and electrical studies of La and Cu doped $BaTiO_3$ ceramics, Physica B 405 (2010) 99–106.
[29] P. Dhak, D. Dhak, M. Das, K. Pramanik, P. Pramanik, Impedance spectroscopy study of $LaMnO_3$ modified $BaTiO_3$ ceramics, Mater. Sci. Eng. B 164 (2009) 165–171.
[30] D.C. Sinclair, A.R. West, Impedance and modulus spectroscopy of semiconducting $BaTiO_3$ showing positive temperature coefficient of resistance, J. Appl. Phys. 66 (1989) 3850–3856.